

# CYBER-PHYSICAL MANUFACTURING METROLOGY MODEL (CPM<sup>3</sup>) APPROACH IN MODELING MILLING AND GEOMETRIC INSPECTION OF TURBINE BLADES

Vidosav MAJSTOROVIĆ<sup>1,\*</sup>, Srdjan ŽIVKOVIĆ<sup>2</sup>

<sup>1)</sup> PhD, Prof., Mechanical Engineering Faculty, Laboratory for Production Metrology and TQM, University of Belgrade, Serbia

<sup>2)</sup> PhD, Experimental Aerodynamics Division, Prototype Production Department, Military Technical Institute Belgrade, Serbia

**Abstract:** *One of the key elements of digital manufacturing is a simulation i.e. virtual modelling of all processes that belong to the manufacturing value chain. This paper aims at estimating the surface deviation error in the free form surfaces machining error and estimate the effect on quality of the measuring process. A set of virtual experiments was designed by applying the central composite design approach of response surface methodology. The first set of virtual experiments determined the optimum tool path strategy. The second set of virtual experiment optimization inspection parameter to achieve maximum measuring accuracy and minimum measuring time. Fully developed methodology was applied to mold turbine blade.*

**Key words:** *virtual optimization, sculptured surface, manufacturing, inspection, digital manufacturing, response surface methodology, mathematical modelling.*

## 1. INTRODUCTION

Today's business structure is more complex and dynamic than ever before. The market requires rapid changes in the industry with new products, which directly reflects on the work of the factory. Information technology (IT) provide new, unimagined possibilities, engineers in the design and planning. These two approaches have led to two concepts that have emerged since then: the digital factory and digital manufacturing [1, 2].

One of the key elements of digital manufacturing (including design-planning-production-inspection value chain) is a simulation i.e. virtual modelling of all processes that belong to the manufacturing chain. Simulations are frequently used to optimize some of the processes of digital manufacturing, in order to improve quality of the process itself and its output.

Modern industrial products impose the application of special manufacturing strategies and methods to meet functionality, quality and aesthetics. Engineering design, modelling, planning and machining of complex mechanical parts that imply sculptural surfaces has been the subject of intensive research for almost three decades. Sculptured surface machining (SSM) [4] is one of those methods widely applied to automotive, consumer electronics and aerospace. Their inspection is directly linked to the development of CMM and related software. Today, development and application of the digital manufacturing concept set up a new basis for this research. In order for these manufacturing technologies to be properly applied, crucial parameters that define them need to be set by

experts and qualified personnel. Driven by the requirement to statistically reduce the parameters involved in terms of their significance ranking two approaches are distinguished: Taguchi's design of experiments (DoE) and response surface methodology (RSM) [2].

Based on the digital product, the interoperability model is developed to integrate design, manufacturing and inspection based on STEP AP242 that was designed to improve the interoperability in STEP manufacturing chain [2]. In an engineering practice, freeform surfaces could be classified as complex geometrical features. According to ISO 17450-1, complex geometrical features have no invariance degree [5].

## 2. VIRTUAL OPTIMISATION OF CAM PROCESS PARAMETERS

RSM allows to trace the "optimum" (or near optimum) response conditions step by step. The first-order design ( $2^k$  factorial, Plackett-Burman, simplex) and second-order design ( $3^k$  factorial, central composite, Box-Behnken) are the most-frequently used approximating polynomial models in classical RSM. The first-order design serves in a preliminary phase to get initial information about the response system and to assess the importance of the factors in a given experiment. The Central Composite Design (CCD) is the most popular of all second-order designs, and is obtained by augmenting a first-order design.

CCD is constructed by two sets of points plus  $\eta C$  centre runs. The former set is a  $2^k$  or a  $2^{k-p}$  resolution fractional factorial design for all factors; whilst the latter set is the  $2^k$  axial runs for each factor with a distance  $\alpha$  from the center.

The aim of the present study is the development of a statistical model which utilizes process parameters found

\* Corresponding author: Kraljice Marije 16, 11120 Belgrade PF34;  
Tel.: + 381 (0)11 33 02 407;  
Fax: + 381 (0)11 33 70 364;  
E-mail addresses: [vidosav.majstorovic@sbb.rs](mailto:vidosav.majstorovic@sbb.rs) (V. Majstorović),  
[srdjan.vti@gmail.com](mailto:srdjan.vti@gmail.com) (S. Živković).

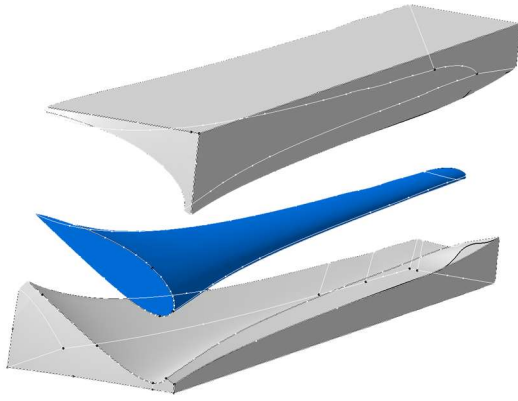


Fig. 1. CAD representation of the wind turbine blade mold components.



Fig. 2. Mold Turbine Blade CAM; 7<sup>th</sup> experimental run.

equation representing the quadratic model in terms of actual factors is showed in Eq. 1.

Response surfaces allow the graphical observation of variations among quality objectives. With reference to the results of machining experiments and the stochastic model generated, three response surfaces for the surface deviation (mm) in relation to the experimental factors cutting speed  $V_C$  (m/min), feed rate  $f$  (mm/min) and cutting direction  $C_D$  ( $^\circ$ deg) are created. Resulting contours examined in response surfaces are in absolute accordance with the results presented earlier through statistical analysis. Fig.2 depicts the response surfaces.

Figure 3 shows response surfaces for model evaluation:  $S_D f(V_C, f)$ , for  $\alpha_e = 30\% \text{ } \emptyset$  and  $C_D = 45^\circ$  (Fig. 3,a);  $S_D f(V_C, C_D)$ , for  $f = 400$  mm/min and  $\alpha_e = 30\% \text{ } \emptyset$  (Fig. 3,b);  $S_D f(f, C_D)$ , for  $V_C = 87.92$  m/min and  $\alpha_e = 30\% \text{ } \emptyset$  (Fig. 3,c);  $S_D f(C_D, \alpha_e)$ , for  $V_C = 87.92$  m/min and  $f = 400$  mm/min (Fig. 3,d);  $S_D f(\alpha_e, V_C)$ , for  $f = 400$  mm/min and  $C_D = 45^\circ$  (Fig. 3,e);  $S_D f(\alpha_e, f)$ , for  $V_C = 87.92$  m/min and  $C_D = 45^\circ$  (Fig. 3,f).

According to ANOVA outputs, the model's  $F$  value (133.68) implies the model is significant, whilst; there is only a 0.01% chance that a "Model  $F$  Value" this large could occur due to noise. Values of "Prob >  $F$ " ( $P$ -value) less than 0.05 verify the significance of model terms. For the process parameters studied, stepover ( $\alpha_e$ ) and the interaction between stepover ( $\alpha_e$ ) and cutting direction ( $C_D$ ) are the most significant model terms ( $F = 1707.6$  with  $P < 0.0001$  and  $F = 5.71$  with  $P < 0.0304$  respectively).  $P$ -values greater than 0.1000 indicate the model terms are not significant. The value for "Pred. R Squared" of 0.9542 is in reasonable agreement with the "Adj. R Squared" of 0.9846. "Adeq. Precision" measures the signal to noise ratio. In general, a ratio greater than 4 is desirable; hence, the ratio of 49.093 indicates an adequate signal hence, it can be used to navigate the design region.

The component which reflected surface finish was that of excess error. Excess error reflects a virtual surface texture indicator showing the material which a tool path may leave uncut due to programming inconsistencies. Table 3 depicts process parameter settings for both approaches together (prediction model and conventional CNC programming on CAM software) with resulting values for the response of surface deviation and excess error.

Note that cutting parameters set for manual approach are very close to the optimal ones proposed by the model so as to strict prediction comparison; yet conform with tool manufacturers' recommendations.

$$S_D = 0.14496 - 6.60392 \cdot 10^{-5} \cdot V_C - 4.45394 \cdot 10^{-6} \cdot f + 6.4936 \cdot 10^{-6} \cdot \alpha_e + 1.145 \cdot 10^{-5} \cdot C_D + 3.8 \cdot 10^{-7} \cdot V_C^2 + 6 \cdot 10^{-9} \cdot f^2 + 3.36 \cdot 10^{-6} \cdot \alpha_e^2 + 1.96 \cdot 10^{-9} \cdot C_D^2 - 6.37 \cdot 10^{-9} \cdot V_C \cdot f + 6.37 \cdot 10^{-8} \cdot V_C \cdot \alpha_e - 1.415 \cdot 10^{-8} \cdot V_C \cdot C_D + 8 \cdot 10^{-9} \cdot f \cdot \alpha_e - 1.78 \cdot 10^{-9} \cdot f \cdot C_D - 3.11 \cdot 10^{-7} \cdot \alpha_e \cdot C_D \quad (1)$$

Table 1

The experiment design summary

Study Type	RSM	Experiments: 30		
Response	Name	Units	Low	High
Y1	$S_D$	mm	Actual Values	
Factor	Name	Units	Low	High
A	$V_C$	m/min	75.4	100.5
B	$f$	mm/min	300	500
C	$\alpha_e$	% $\emptyset$ , mm	20	40
D	$C_D$	$^\circ$ deg	0	90

in typical CAM software such as cutting speed, feed rate, step-over and cutting direction to investigate the regions for optimal parameter settings for surface finish optimization. Experiments were carried out in the form of simulations for the machining of a wind turbine blade mold component (Fig. 1) under different conditions according the number of experiments [6]. Thereby, a predictive model for surface deviation is developed by taking advantage of ANOVA (Analysis of Variance) statistical values. RSM is exploited to conduct the experiments.

The machining parameters treated as independent variables were cutting speed  $V_C$ , feed rate  $f$ , step-over  $\alpha_e$  and cutting direction  $C_D$ . The response was the surface deviation (SD) that occurs between the machined and the ideally designed 3D CAD model surface. Machined part is facet body (STL) obtained by generating IPW (In Process Work piece). The IPW is a geometric shape that is produced by the Manufacturing application to represent the machined work piece at each stage of machining. Using Deviation Gauge command system display deviation data between target objects (IPW) and one or more reference objects (model surfaces). The most often used class of designs to fit higher order polynomials is the central composite design (CCD). CCD is constructed by two sets of points plus center runs [8]. Experiment design summary after applying CCD to CAM software machining parameters is given in table 1, showing minimum and maximum value of chosen variables.

Total number of experiments is 30. Figure 2 shows 7<sup>th</sup> experimental runs. Cutting speed  $V_C$  (depends of cutter diameter & spindle rpm) and federate  $f$  (depends of feed per tooth, num. of tooth & spindle rpm) are not completely independent variables. ANOVA results final

Table 2

A part of CCD experimental design addressing 4 machining parameters and obtained response

Run	Cutting Speed (m/min)	Feed rate (mm/min)	Radial Cut $a_e$ (% $\emptyset$ , mm)	Cut Direction ( $^\circ$ deg)	Machined Surface Area (mm <sup>2</sup> )	Target Surface Area (mm <sup>2</sup> )	$S_D$ Actual (mm)	$S_D$ Predicted (mm)
1	100.48	500	20	90	280842.7822	280497.904	0.000614383	0.00112
2	75.36	500	20	0	280673.5882		0.000313067	0.00098
...	...	...	...	...	...		...	...
29	100.48	500	20	0	280673.5882		0.000313067	0.00086
30	100.48	500	40	90	283115.687		0.004644641	0.00394

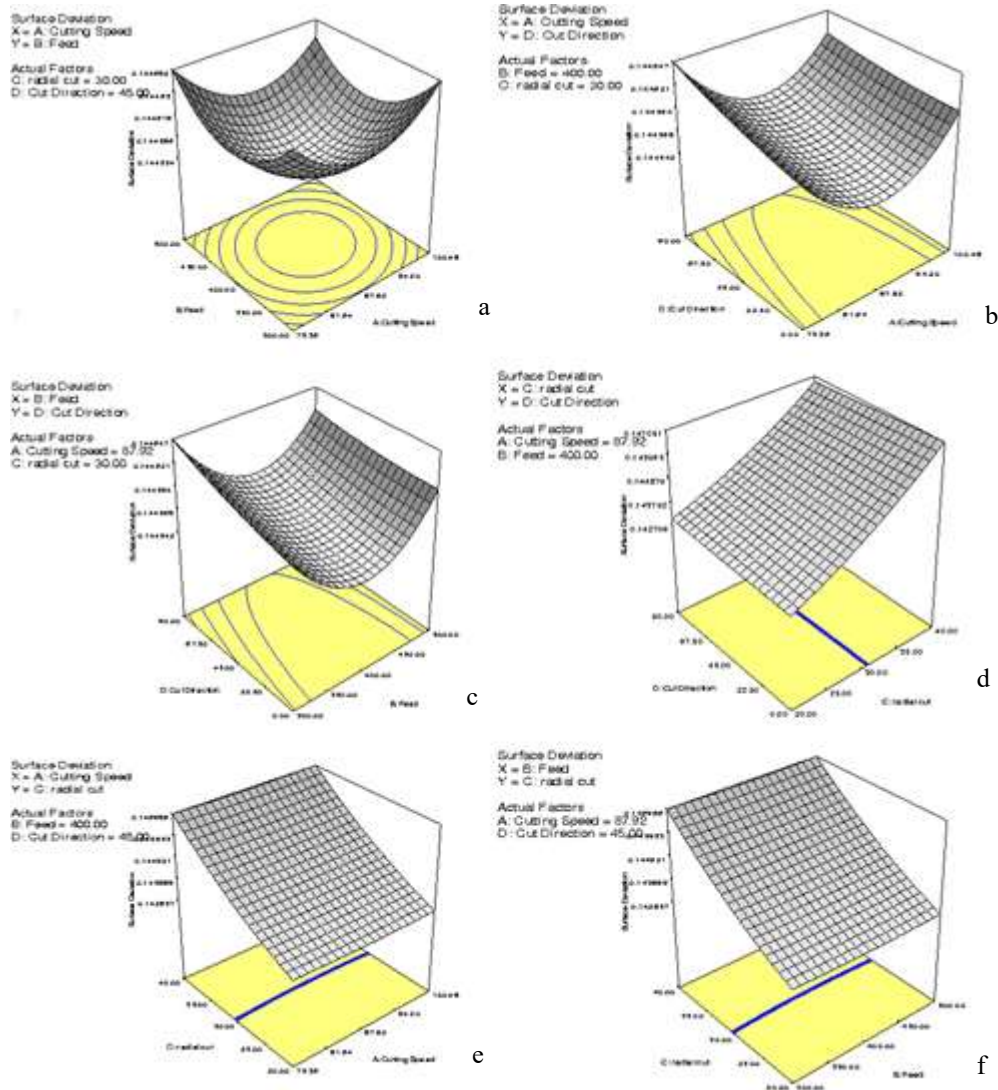


Fig. 3. Response surfaces for model evaluation [6]: a –  $S_D f(V_C, f)$ , for  $a_e = 30\% \emptyset$  and  $C_D = 45^\circ$ ; b –  $S_D f(V_C, C_D)$ , for  $f = 400$  mm/min and  $a_e = 30\% \emptyset$ ; c –  $S_D f(f, C_D)$ , for  $V_C = 87.92$  m/min and  $a_e = 30\% \emptyset$ ; d –  $S_D f(C_D, a_e)$ , for  $V_C = 87.92$  m/min and  $f = 400$  mm/min.

Table 3

Parameter settings and obtained results for quality objectives

Prediction model (desirability for solution: 0.875) with CAM software					
Process parameters - settings				Responses	
$V_C$ (m/min)	$f$ (mm/min)	$a_e$ (% $\emptyset$ , mm)	Cutting direction ( $^\circ$ deg)	Surface deviation (mm)	Excess error (mean value)
87.04	433.46	22.54% (2.25 mm)	52.89	Predicted: 0.00047	0.28
Conventional CNC programming with CAM software					
Process parameters - settings				Responses	
$V_C$ (m/min)	$f$ (mm/min)	$a_e$ (% $\emptyset$ , mm)	Cutting direction ( $^\circ$ deg)	Surface deviation (mm)	Excess error (mean value)
80	430	2	0	0.00053	0.34

### 3. VIRTUAL OPTIMISATION OF CAI PROCESS PARAMETERS

Our focus is on the development of a virtual CAI (Computer Aided Inspection) model based on CAD, that enables the inspection plan definition for complex, freeform surfaces of real parts inspected after the machining on CNC machines.

Today there are two general approaches for the measurement of freeform shaped parts: direct and indirect comparison [4]. The basic principle of direct comparison is to check the degree of deviation between the surface and master templates. In our case, these masters represent two-dimensional cross-sections of the surface to be inspected in a virtual CAD model. In freeform metrology it is fundamental to measure a large number of points and cross-sections distributed on the surface [5].

The inspection planning is the most important step in the development of CAI model [5] for a freeform surface. In a context of the research presented in this paper, the most important approach is STEP and STEP-NC enabled inspection. Starting from STEP AP219, AP224, AP238 and AP242, CMM generates an inspection plan in DMIS (Dimensional Measuring Interface Standard – ISO 22093) format.

The most important parameters of sculptured surfaces inspection on CMM are adopted as control factors in this experiment: number of control sections [ $N^{\circ}CS$ ], number of measuring points in the control sections [ $N^{\circ}MP$ ], and measuring points' distribution along the control sections [ $DistrMP$ ]. As it could be seen from Table 4, control factor  $N^{\circ}CS$  is varied on 5 levels (3,6,10,14 and 18 control sections), factor  $N^{\circ}MP$  on 5 levels (6, 11, 15, 21 and 41 measuring points in a control section), and  $DistrMP$  on 2 levels: uniform [ $u$ ] distribution (equal parameters along the curve), and the distribution with geometric progression ratio of 1.2 [ $g$ ]. The selection of values for  $N^{\circ}CS$ ,  $N^{\circ}MP$  and  $DistrMP$  was based on previous research in freeform surfaces coordinate inspection (e.g. [4, 5]).

Virtual coordinate inspection of the lower segment of a mold turbine blade (MTB) was performed on a virtually machined part. Machined part is represented by the STL file obtained as a result of the machining simulation explained in first part of research. Nominal MTB geometry was transferred from the CAD/CAM system used for simulation of the measurements. The surface of MTB has been defined using a mesh of 18 main control sections, as shown in figure 4. Real MTB geometry presented by STL file has been obtained by choosing 28<sup>th</sup> run of total 30 different machining strategies [6], as explained in chapter 2. Theoretical coordinates ( $X_T$ ,  $Y_T$ ,  $Z_T$ ) are the obtained from the STEP file, measured coordinates are

obtained from STL ( $X_M$ ,  $Y_M$ ,  $Z_M$ ). Deviation presents the shortest distance between the theoretical and the measured  $DistrMP$ , the inspection curves are fitted using cubic splines. In the virtual experiment, the number of control sections ( $N^{\circ}CS$ ) was varied from 3 to 18, to create a sheet body of the inspected part (MTB).

Figure 4 depicts position and distribution of control section, used for simulation of coordinate inspection.

#### 3.1. Experimental Plan and Responses

Since the number of levels is different for the control factors used in the experiment, the factorial design (with no replicates) is selected in order to design the experimental plan. As a result, the generated experiment plan contains 50 experimental runs.

Measuring accuracy is the most important indicator of CAI process quality. In this experiment, it is presented by the following characteristics (Table 5):

- Distance Error:  $DE_{mean}$  and  $DE_{stdev}$ ;
- Angle Error:  $AE_{mean}$  and  $AE_{stdev}$ .

Since the main objective is to maximize the measuring accuracy, it is explicit that the goal is to achieve minimal  $DE_{mean}$  and  $AE_{mean}$ , and also to reduce their variation  $DE_{stdev}$  and  $AE_{stdev}$ . Measuring time, presented over the probe path length (response  $L$ ) is also observed with the objective to minimize it. Therefore, in total, five characteristics are observed as responses from the virtual experiment.

Table 4

Control factors and levels used in the experiment

Control Factors	Levels				
	1	2	3	4	5
$N^{\circ}CS$	3	6	10	14	18
$N^{\circ}MP$	6	11	15	21	41
$DistrMP$	$u$	$g$	-	-	-

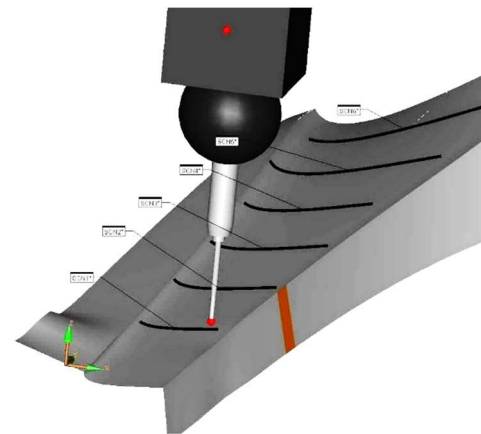


Fig. 4. MTB control sections and CMM simulation.

Table 5

A part of experimental plan and obtained response characteristics

Run.	Control factors			Responses				
	$N^{\circ}MP$	$N^{\circ}CS$	$DistrMP$	$DE_{mean}$ [mm]	$DE_{stdev}$ [mm]	$AE_{mean}$ [°]	$AE_{stdev}$ [°]	$L$ [m]
1	6	18	uniform	0.2219	0.3547	2.6185	5.2357	3.9
2	6	14	uniform	0.2331	0.3467	2.7486	5.4246	3.2
...	...	...	...	...	...	...	...	...
49	41	14	geometric	0.0883	0.0965	0.9068	2.7649	11
50	41	10	geometric	0.1053	0.1546	0.9603	2.6339	8

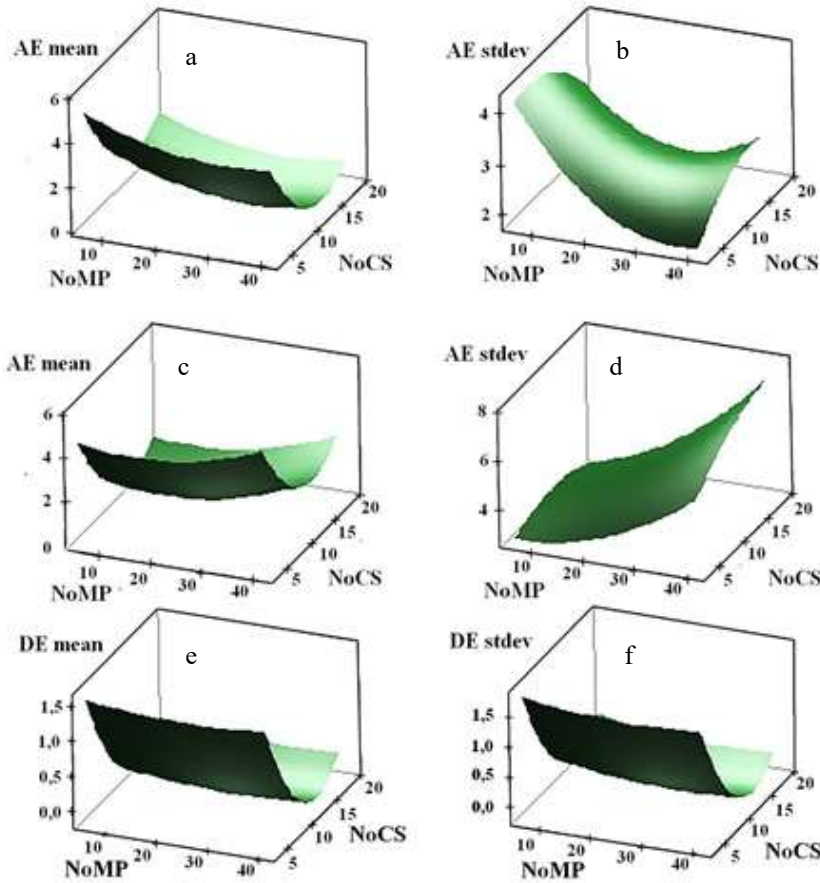


Fig. 5. Surface plots for the responses [7].

In order to assess the effects of CAI parameters on the observed characteristics, the analysis was performed using RSM. Analysis of variance (ANOVA) for responses  $DEmean$ ,  $DEstdev$ ,  $AEmean$ ,  $AEstdev$  and  $L$  are a full quadratic model (second order model) has been considered for all responses. The adequacy of regression models was evaluated using  $R^2$  value that shows how close the actual data are to the fitted regression curve. It is important to mention that the  $R^2$  statistic, which in this case presents percentage of variation in a response explained by the observed control factors, is over 90% for all responses. This confirms validity of the statistical analysis that follows. The corresponding regression formulas are given separately for the uniform ( $u$ ) and the distribution with geometric progression ( $g$ ), respectively [7]; equation 2–10.

$$DEmean_u = 2.688 - 0.012 NoMP - 0.404 NoCS + 0.0003 NoMP^2; \quad (2)$$

$$+ 0.015 NoCS^2 - 0.00008 NoMP \cdot NoCS$$

$$DEmean_g = 2.602 - 0.010 NoMP - 0.402 NoCS + 0.0002 NoMP^2; \quad (3)$$

$$+ 0.015 NoCS^2 - 0.00008 NoMP \cdot NoCS$$

$$DEstdev_u = 3.071 - 0.018 NoMP - 0.441 NoCS + 0.0003 NoMP^2; \quad (4)$$

$$+ 0.016 NoCS^2 - 0.0001 NoMP \cdot NoCS$$

$$DEstdev_g = 2.951 - 0.014 NoMP - 0.440 NoCS + 0.0003 NoMP^2; \quad (5)$$

$$+ 0.016 NoCS^2 - 0.0001 NoMP \cdot NoCS$$

$$AEmean_u = 8.546 - 0.133 NoMP - 0.953 NoCS + 0.002 NoMP^2; \quad (6)$$

$$+ 0.035 NoCS^2 + 0.0007 NoMP \cdot NoCS$$

$$AEmean_g = 7.365 - 0.069 NoMP - 0.931 NoCS + 0.002 NoMP^2; \quad (7)$$

$$+ 0.035 NoCS^2 + 0.0007 NoMP \cdot NoCS$$

$$AEstdev_u = 5.020 - 0.193 NoMP + 0.062 NoCS + 0.003 NoMP^2; \quad (8)$$

$$- 0.007 NoCS^2 + 0.004 NoMP \cdot NoCS$$

$$AEstdev_g = 2.520 - 0.049 NoMP + 0.141 NoCS + 0.003 NoMP^2; \quad (9)$$

$$- 0.007 NoCS^2 + 0.004 NoMP \cdot NoCS$$

$$L_{u,g} = 509.0 + 9.33 NoMP + 105.88 NoCS - 0.09 NoMP^2 - 0.74 NoCS^2 + 15.65 NoMP \cdot NoCS \quad (10)$$

Since the experiment considered five responses, it is necessary to select the optimal values of CAI control factors in order to maximize measuring accuracy (i.e. minimize  $DEmean$ ,  $DEstdev$ ,  $AEmean$ ,  $AEstdev$ ) and minimize measuring time (i.e. minimize  $L$ ). It has been mentioned that the regression models for all responses are adequate, so the analysis of surface plots can indicate the optimal control factor settings.

Fig. 5 shows surface plots for the responses  $AEmean$  (a),  $AEstdev$  (b) for uniform distribution;  $AEmean$  (c),  $AEstdev$  (d) and distribution with geometric progression;  $DEmean$  (e), and  $DEstdev$  (f), for the uniform distribution.

In order to identify the control factors setting that simultaneously fulfil requirements for all responses, a response optimizer (superposition plot) is generated. First, each response is converted into a desirability function (that takes values from 0 to 1), and then the composite desirability function is calculated as the geometric mean of the individual desirability functions. In this experiment, the obtained solution must satisfy the requirements to minimize all five responses. Since for the quality of CAI process the measuring accuracy (presented by distance error and angle error) is more important than the measuring time (presented over the value  $L$ ), the importance of responses that describe the measuring accuracy is set to 5, and the importance of response  $L$  that describes inspection time is 1. Results of simultaneous optimization, in terms of the optimal control factors setting, are:  $N^oCS = 17$ ;  $N^oMP = 24$ ;  $DistrMP = \text{uniform}$ ; the composite desirability equals 0.87, so the obtained solution is accepted.

The desirability for individual responses are: for  $DEmean$ ,  $DEstdev$  and  $AEmean$  the desirability equals 1 (the ideal value);

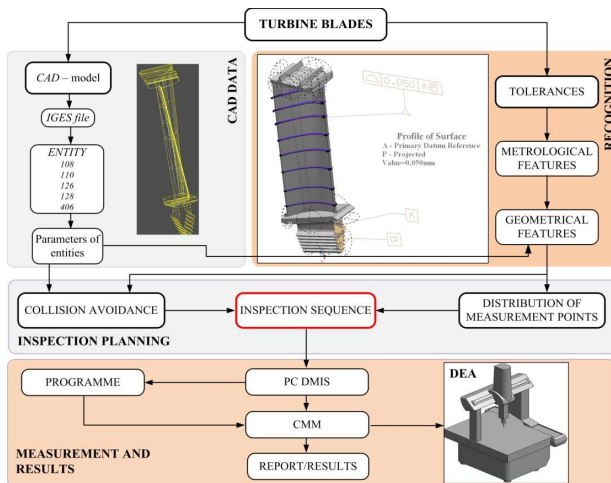


Fig. 6. CPM<sup>3</sup> – Inspection planning of turbine blades [9].

for  $A_{Estdev}$  the desirability value equals 0.75 which is acceptable; and for the response  $L$  the desirability equals 0.44 which could be expected since the importance of  $L$  is set to be five times smaller than for the other responses. The suggested control factors setting is adopted as the optimal solution of the observed problem – CAI of a mold turbine blade (MTB).

#### 4. OUR RESEARCH IN THE FIELD OF CYBER-PHYSICAL MANUFACTURING METROLOGY MODEL (CPM<sup>3</sup>)

The framework of our CPM<sup>3</sup> model is presented in Fig. 6. It consists of the following sub-modules:

- Module for recognition of geometrical features from CAD/GD&T model of the measurement part;
- Intelligent inspection process planning module,
- Coordinate measuring machine (CMM) – generation of control data list for CMM that is transferred to CMM using cloud technology, and
- Module for analysis of results and generation of the reports.

Cloud services within the company provide the necessary information for integration of knowledge and data from various phases in product design and manufacturing into inspection planning, and make available information about inspection results to all interested parties in product lifecycle.

Geometrical features recognition module recognizes features from 3D model of measurement part in a neutral CAD format, usually STEP. Geometrical features of interest depend on the type of measurement part and the applied standards. If recognition module does not have the application for recognition of the geometrical features for the considered measuring part in its database, the application for features recognition needs to be provided along with the part model.

#### 5. CONCLUSION

In the first part of the research RSM is used to assess virtual machining quality via the prediction of Surface Deviation as a target objective. A series of experiments conducted following a CCD having as independent variables cutting speed  $V_c$  (m/min), feed rate  $f$  (mm/min), radial cut  $a_e$  (% $\phi$ ) and cutting direction CD ( $^\circ$ deg). A quadratic model was developed to relate the response with machining parameters. ANOVA and statistical analysis revealed that the quadratic model generated was significant ( $F$  value = 133.68), thus it can be used to predict

surface deviation among designed and machined models in CAM.

In the second part of the research RSM is used to assess the effect of CAI control factors ( $N^{\circ}CS$ ,  $N^{\circ}MP$ , and  $DistrMP$ ) on the quality of measuring process (measuring accuracy and measuring time). The measuring accuracy is presented by the distance error and the angle error, and the measuring time is presented by the measuring path length. The results of analysis performed using RSM are:  $N^{\circ}CS$  and its square term are significant for the distance error; all three control factors and/or their square terms and interactions are significant for the angle error; for the measuring path length only  $DistrMP$  is insignificant.

Our research in the field cyber-physical manufacturing metrology model (CPM<sup>3</sup>) presented in this paper was concentrated on the:

- defining CPM<sup>3</sup> model and its structure,
- development of a model knowledge base for this model, for chosen example, and
- the establishment of total hardware and software configurations.

The next steps of this research are:

- developing software structure of the virtual part of the model,
- testing the IoT elements for this model.

#### REFERENCES

- V. Majstorović, *Manufacturing Innovation and Horizon 2020 –Developing and Implement "New Manufacturing"*, Journal of Proceedings in Manufacturing Systems, Vol. 9, Issue 1, 2014, pp. 3–8.
- V. Majstorović, J. Mačužić, S. Stojadinović, S. Živković, T. Šibalija, V. Marinkovic, *Cyber Physical Manufacturing – Integrated Quality Approach*, Proceedings of 6<sup>th</sup> International Symposium on Industrial Engineering SIE 2015, Belgrade, September 2015, pp. 137–140.
- V. Majstorović, J. Mačužić, T. Šibalija, S. Živković, *Cyber-Physical Manufacturing Systems – Manufacturing Metrology Aspects*, Journal of Proceedings in Manufacturing Systems, Vol. 10, No. 1, 2015, pp. 9–14.
- J. Makem, H. Ou, C. Armstrong, *A virtual inspection framework for precision manufacturing of aerofoil components*, Computer-Aided Design, Vol. 44, Issue 9, September 2012, pp. 858–874.
- S. Živković, *Coordinate metrology in manufacturing of the complex spatial forms with applications to the aerodynamic surfaces*, Military Technical Institute, Belgrade, 2014.
- N. Fountas, T. Šibalija, V. Majstorović, J. Mačužić, S. Živković, N. Vaxevanidis, *Virtual Quality Assessment for Sculptured Surface CNC Tool Path Strategies and Related Parameters Using RSM and Developed Model for Inspection*, Proceeding of the 8<sup>th</sup> International Working Conference TQM –Advanced and Intelligent Approaches, Belgrade, June 2015, pp. 203–214.
- T. Šibalija, S. Živković, N. Fountas, V. Majstorović, J. Mačužić, N. Vaxevanidis, *Virtual optimization of CAI process parameters for the sculptured surface inspection*, Procedia CIRP, Vol. 57C, 2016, pp. 574–579.
- D.C. Montgomery, *Design and Analysis of Experiments*, 7<sup>th</sup> edition, Wiley and Sons, 2009.
- V. Majstorović, S. Stojadinovic, S. Živković, D. Djurdjanovic, Z. Jakovljevic, N. Gligorijevic, *Cyber-Physical Manufacturing Metrology Model (CPM<sup>3</sup>) for Sculptured Surfaces – Turbine Blade Application*, Procedia CIRP, Vol. 63, 2017, pp. 658–663.